Easy Calibration of a Head-Mounted Projective Display for Augmented Reality Systems

Chunyu Gao[1], Hong Hua[1,2], and Narendra Ahuja[1]
[1]*Beckman Institute, University of Illinois at Urbana-Champaign, Urbana, IL 61801*
[2]*Department of Information and Computer Science, University of Hawaii at Manoa, Honolulu, HI 96822*
Email: Hhua@hawaii.edu

Abstract

Augmented reality (AR) superimposes computer-generated virtual images on the real world to allow users exploring both virtual and real worlds simultaneously. For a successful augmented reality application, an accurate registration of a virtual object with its physical counterpart has to be achieved, which requires precise knowledge of the projection information of the viewing device. This paper proposes a fast and easy off-line calibration strategy based on well-established camera calibration methods. Our method does not need exhausting effort on the collection of world-to-image correspondence data. All the correspondence data are sampled with an image based method and they are able to achieve sub-pixel accuracy. The method is applicable for all AR systems based on optical see-through head-mounted display (HMD), though we took a head-mounted projective display (HMPD) as the example. In this paper, we first review the calibration requirements for an augmented reality system and the existing calibration methods. Then a new view projection model for optical see through HMD is addressed in detail, and proposed calibration method and experimental result are presented. Finally, the evaluation experiments and error analysis are also included. The evaluation results show that our calibration method is fairly accurate and consistent.

1. Introduction

The promise of an augmented reality (AR) system lies in the coexistence of virtual and real information with which users can not only naturally interact with a real world but also have sensory access to knowledge associated with it. . Several researchers have been exploring potential AR applications. For example, Feiner and his colleagues developed a laser printer maintenance tool using 3D interactive techniques [9]. A group in Boeing tried to use a see-through HMD to guide the technician on manufacturing and assembly processes [5]. Other applications include computer–aided surgery [3, 20], medical training [1] and tele-manipulation [21].

However, the registration between physical and computer-generated objects is still a challenging issue. In order to achieve a registration with acceptable accuracy, the following factors have to be considered:

1) The intrinsic and extrinsic parameters of the viewing system, through which both the physical and virtual objects are viewed;
2) The transformations matching virtual world coordinates with their real counterparts, through which virtual components are placed with respect to their world reference;
3) The resolution and accuracy of the motion tracking systems, through which a user's head and objects of interest are tracked to update their corresponding transformations;
4) The end-to-end system latency, which refers to the time delay from the moment when an interaction takes place to the moment when the corresponding properties of the synthetic world are updated.

The first three factors are identified as the sources of static registration errors because they result in mis-registration even if a user is still. The last factor is typically identified as the source of dynamic registration error because it only plays a role in a dynamic environment. The focus of this paper is to present a fast and easy off-line calibration method to improve static registration in a custom-designed augmented reality system, which is based upon head-mounted projective display (HMPD) technology [8, 11, 19]. With minor modifications, the proposed method can be adapted for other optical see-through HMDs.

The rest of the paper is organized as follows: We first briefly review related work in calibration methods and our motivations in section 2. Then in section 3, we concisely summarize the basic concept and recent advancement in the HMPD technology and calibration requirements. In section 4, we present a new projection model and the proposed calibration method and include the calibration procedures and experimental results. Finally, an evaluation experiment and results are included in section 5.

Proceedings of the IEEE Virtual Reality 2003 (VR'03)
1087-8270/03 $17.00 © 2003 **IEEE**

2. Related work and motivation

Calibration has been an important research subject in AR. Deering presented the general steps that must be taken to produce accurate high-resolution head-tracked stereo display in order to achieve sub-centimeter virtual-to-physical registration [7]. Azuma and Bishop described experimental steps to estimate viewing parameters and presented predictive tracking techniques to improve both static and dynamic registration in an optical see-through HMD [2]. Janin et al. proposed both direct measurement and on-line optimization methods to calibrate an optical see through HMD[17]. Oishi and Tachi proposed a calibration method to minimize systematic errors in projection transformation parameters to improve registration accuracy [22]. Tuceryan and Navab described a single point active alignment method (SPAAM) for optical see-through displays [27]. The calibration of video-based and monitor-based AR systems has been addressed in [4, 10, 26].

For most of these calibration methods, the accuracy of data sampling (e.g. world-to-image correspondence matching) is always critical, which is limited by the accuracy of matching methods and available head trackers. In our earlier work [15], we described a manual correspondence matching (MCM) strategy to calibrate an HMPD prototype, in which the accuracy of world coordinate measurements is about a few millimeters or even up to a centimeter. We studied the relationship between data sampling conditions and the convergence and accuracy of the MCM method. We find that, for each arm of the HMD optics, more than 300 samples are needed to achieve a stable and accurate convergence, while we made 1080 samples to study the relationship. This task is a very tedious and time-consuming work for a trained user and is even impossible for an untrained user. However, camera calibration methods, which are well-established in computer vision domain, determine the world-to-image matching by automatic feature detection algorithms that could sample hundreds of points in less than one second with sub-pixel accuracy. The key difference of a camera calibration from a display calibration is the fact that a camera has digital access to the physical world. In order to take advantage of the automatic matching algorithms used by camera calibration, a different strategy is necessary. Our aim is to minimize the accuracy limitation implied by tracking system, improve the accuracy of world-to-image correspondence matching, and minimize the necessary efforts. In this paper, we propose an automatic correspondence matching (ACM) approach, in which we calibrate two cameras using established camera calibration methods and then infer the intrinsic and extrinsic parameters of the viewing device using the images of the display captured by the calibrated cameras.

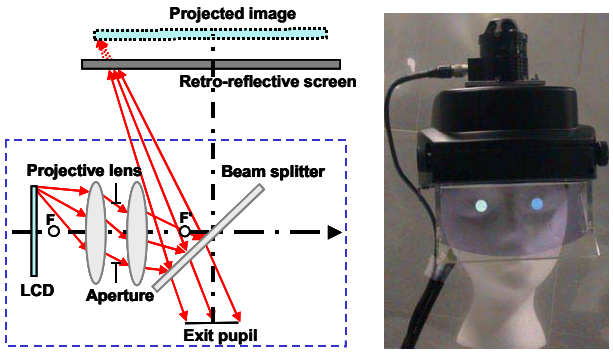

(a) (b)

Fig.1 Head-mounted projective display (HMPD) (a) Illustration of basic imaging concept with a monocular configuration; (b) Prototype implementation.

3. Calibration requirements

In this section, we briefly review the HMPD technology and calibration requirements for an AR system.

3.1. Overview of the HMPD technology

Video and optical see-though HMDs have been the two basic approaches to combining real and virtual images [24]. In both approaches, the viewing optics typically is eyepiece-type compound magnifier. The HMPD is an emerging technology that can be thought to lie on the boundary of conventional HMDs and projective displays such as the CAVE systems [6].

An HMPD consists of a pair of miniature projection lenses, beam splitters, and displays mounted on the head and a supple retro-reflective screen placed strategically in the environment [11]. Its monocular configuration is illustrated in Figure 1-a. Rays from the miniature display, which is located beyond the focal point of the lens rather than between the lens and the focal point as in a conventional HMD, are projected through the lens and retro-reflected back to the exit pupil, where a user's eye is positioned to observe the magnified virtual image. Because of the retro-reflective property, in which a ray hitting the surface is reflected back on itself in the opposite direction, the location and size of the perceived image are independent of the location and shape of the retro-reflective screens [11].

The HMPD concept has been recently demonstrated to yield 3D visualization capabilities with a large-FOV, lightweight and low distortion optics, and correct occlusion of virtual objects by real objects [12, 13, 14, 16, 18]. Thus, the HMPD technology was identified as an alternative to optical see-though HMDs for augmented applications [23]. The prototype used in our AR system is showed in figure 1-b [13].

3.2 Calibration requirements for registration of virtual and real objects

Figures 2-a and 2-b illustrate the main components, the associated coordinate systems, and the transformations in the physical and virtual worlds, respectively. In the virtual environment, we define a virtual world coordinates (VWC), W_VXYZ. Two virtual cameras are properly placed in the VWC to generate the 2D projections of a 3D world. Given a 3D point $P_{W_V}(x_{wv}, y_{wv}, z_{wv}, 1)$ in the VWC, its 2D projection $p_{I_v}(x_{iv}, y_{iv}, w_{iv})$ on the viewing plane of a virtual camera is given by

$$p_{I_v} = M_{C_v} T_{C_v \leftarrow W_V} P_{W_V} \quad (1)$$

The corresponding viewport coordinates (u, v) are $u = x_{iv}/w_{iv}$ and $v = y_{iv}/w_{iv}$, respectively. $T_{C_v \leftarrow W_V}$ is a rigid transformation that transforms a 3D point from the world reference to the virtual camera reference, and M_{C_v} represents the imaging properties of the virtual camera.

In the real world, we define a physical world coordinates (PWC), W_PXYZ. Through a viewing device such as the HMPD, a user's eye observes the superposition of the projections of both a virtual object and its physical counterpart. Given a 3D point $P_{W_P}(x_{wp}, y_{wp}, z_{wp}, 1)$ in the PWC, its 2D projection $p_{I_P}(x_{ip}, y_{ip}, w_{ip})$ on the display window of the viewing system is given by

$$p_{I_p} = M_E T_{E \leftarrow W_p} P_{W_p} \quad (2)$$

where $T_{E \leftarrow W_p}$ is a rigid transformation that transforms a 3D point from the world reference to the eye reference $EXYZ$, and M_E represents the imaging properties of the viewing device.

To superimpose the virtual environment precisely on the real environment, the virtual cameras should be positioned and orientated in the same way as the user's eyes in the real world, and their imaging parameters should match with those of the viewing device, given the assumption that the virtual world reference is well aligned with the real world reference, that is, $T_{C_v \leftarrow W_v} = T_{E \leftarrow W_p}$ and $M_{C_v} = M_E$. The first part is referred to as the extrinsic viewing orientation transformation, and the second part as the intrinsic viewing projection transformation.

The viewing orientation transformation can be further decomposed and expressed with its correspondence in the PWC:

$$T_{C_V \leftarrow W_V} = T_{E \leftarrow W_P} = T_{E \leftarrow S} T_{S \leftarrow W_P} \quad (3)$$

where $T_{S \leftarrow W_P}$, referred to as sensor transformation, is measured explicitly by the head tracker, and $T_{E \leftarrow S}$, referred to as eye transformation, specifies the eyepoint position and viewing orientation in the sensor coordinates.

The key of the HMPD calibration is to estimate the viewing projection matrix M_E that is used to specify the imaging properties of a virtual camera and the eye transformation $T_{E \leftarrow S}$ that is used to define the position and orientation of a virtual camera with respect to the sensor reference of the head tracker.

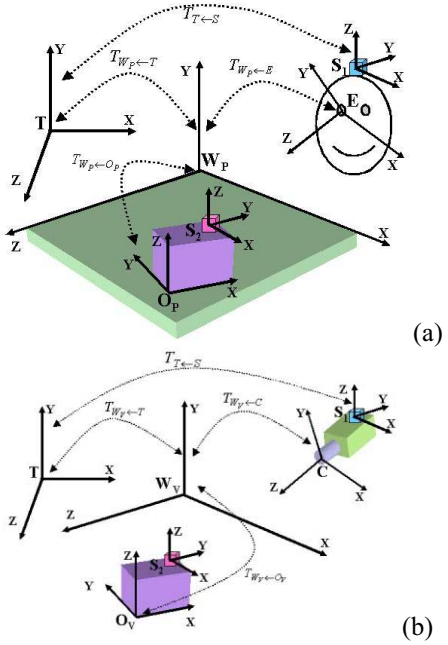

Fig. 2 Illustration of the physical and virtual world components and transformations: (a) Physical world illustration; (b) Virtual world illustration.

4. Proposed off-line calibration method

4.1 Modeling the HMPD viewing system

The nature of the HMPD viewing optics is a camera-type projection system: the image displayed on the LCD screen is projected through the projection lens to form a real image in the physical world space, and a user views the image at the exit pupil of the display. Therefore, the HMPD viewing system presents a two-step projection process, through the projection lens and through the human eye. The projection center O of the HMPD viewing optics and the eyepoint E are theoretically overlapped but in practice they might have small difference for different users. Figure 3 illustrates a practical viewing configuration in which the eyepoint E is slightly displaced from the projection center O. We define an equivalent viewing projection (EVP) system which encompasses the two-step projection. E is the

projection center and coincides with eyepoint. The Z axis of the EVP reference is normal to the display image plane. We define a normalized image plane P_n, which has the same window size as that of the LCD and is parallel with the LCD plane as well as the image plane. Under this circumstance, the equivalent focal length of the EVP system can be defined as the distance from eye position to this normalized plane P_n. The center offset (u_0, v_0) is defined as the offset of the intersection of EVP Z-axis with the normalized plane P_n from the display origin I. The aspect ratio (α, β) and distortion coefficient (K_1) are closely related to the pixel size of LCD screen and the optical properties of the projection lenses, respectively.

Based on the analysis in the previous section, in order to accurately model the virtual cameras used to generate the 2D projections, we need to estimate the extrinsic eye transformation $T_{E\leftarrow S}$ with respect to the sensor reference to form viewing orientation transformation of virtual cameras. We also need to estimate the intrinsic projection transformation M_E of the viewing systems to model the imaging properties of the virtual cameras. In fact, the EVP is the effective viewing system we use to configure the virtual cameras. $T_{E\leftarrow S}$ can be decomposed as a pure rotation R_E and a pure translation T_E. With respect to the sensor reference, indeed, the rotation R_E defines the orientation of the EVP reference and the translation T_E specifies its location. M_E is defined by the equivalent projection parameters and is given by:

$$M_E = \begin{bmatrix} -\alpha f & 0 & u_0 \\ 0 & -\beta f & v_0 \\ 0 & 0 & 1 \end{bmatrix} \qquad (4)$$

It is important to realize that these display intrinsic parameters may slightly change due to their dependence on eye position when a user wears the display. This dependence makes the display projection transformation different from that of a camera system, which remains fixed.

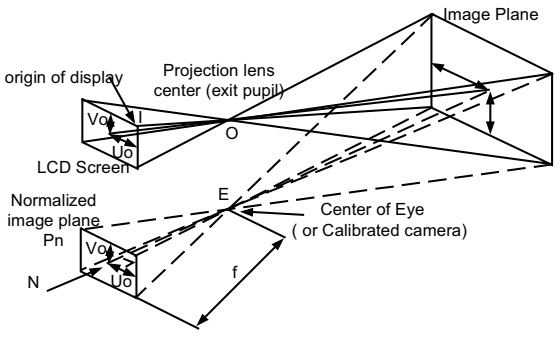

Fig.3 Two-step projection in HMPD system

4.2 Calibration method

In our previous work, we presented a manual correspondence matching (MCM) method to locate sufficient number of world-image correspondences and estimate the extrinsic and intrinsic display parameters using well-established least-square fitting algorithms [15]. The world-image correspondences are manually determined point by point and the world coordinates of the samples are measured manually as well. The MCM method needs more than 300 correspondence samples to achieve stable and accurate convergence. It is time and labor consuming.

In this paper, we present an easy and fast off-line calibration method, referred to as automatic correspondence matching (ACM). In the ACM method, for each arm of the HMPD viewing optics, a calibration camera, which is used to mimic a user's eye, is mounted at the eyepoint position E (close to the corresponding exit pupil of the HMPD and approximately aligned with the optical axis of the display). Then using an established camera calibration method, we estimate the intrinsic and extrinsic parameters of each calibration camera. Generally, the extrinsic parameters give us the relationship between the calibration board reference and the camera reference. If we can obtain the transformation from the calibration board reference to the world reference as well as the transformation of the head tracker, we can calculate the position and orientation of the calibration camera in the sensor reference. While the estimated camera orientation is different from the orientation R_E of the eye transformation, the camera position in the sensor reference gives the position estimate T_E of the eye transformation. The next step is to display a calibration pattern (e.g. a black-white checker pattern) on the LCD of the HMPD. Using the calibrated camera, we capture an image of the magnified calibration pattern formed through the HMPD optics. This captured image includes the intrinsic and extrinsic parameters of EVP system we need to estimate. The display-to-image correspondences are determined using image-based feature detection algorithms. Given the physical size of those grid patterns on the LCD screen and the estimated parameters of the calibration camera, we can inversely estimate the location and orientation of the normalized image plane in the calibration camera reference. Using the estimates, we then compute the orientation R_E of the EVP reference in the sensor coordinates, the effective focal distance f, and the center offset (u_0, v_0). To estimate the distortion coefficient of the viewing optics, there are two approaches [28]:

1). Estimating the radial distortion by alternation: When the distortion of projection lens is fairly small, we can estimate other parameters first, and then recursively apply a variable amount of distortion on the undistorted calibration pattern and re-estimate all the parameters

until the overall error is minimized. We adopted this method in our experiment.

2). Maximum likelihood non-linear search: If the lens distortion is expected to be fairly large, the first approach may not work well. In this case, one may calculate distortion factor using Maximum Likelihood Estimation. The distortion is not merely a linear problem, thus a non-linear search for global minimum has to be applied. We did not apply this method due to lens distortion in our system is neglectable.

4.3. Calibration procedures and results

The calibration implementation consists of the following steps:

1) Mount the HMPD and two calibration cameras (one for each optics) on a fixed platform, record the measurement of the head sensor, and obtain the corresponding sensor transformation $T_{S\leftarrow W_P}$. Empirically, when only one sensor is used for both head tracking and stylus measurement, the sensor measurement should be recorded at the end of the experiments;
2) Calibrate the cameras using selected camera calibration methods [25, 28], and obtain the intrinsic and extrinsic parameters of each camera. In experiments, we used Zhang's method [28];
3) Capture the image of an extra camera calibration board and calculate the attitude of the board in the camera reference to obtain the transformation $T_{B\leftarrow C}$ from the calibration camera reference C to the board reference B. More extra boards can be used to improve accuracy;
4) Measure selected points on the extra calibration board using the tracking stylus to obtain the transformation $T_{W_P\leftarrow B}$ from the board reference to the world reference. The methods used to form $T_{W_P\leftarrow B}$ can be found in our previous calibration paper [15];
5) Display a calibration pattern (e.g. a black-white checker pattern) on the LCD of the HMPD and capture an image using the calibrated cameras. The display-to-image correspondences are determined using image-based feature detection algorithms (Fig. 4).
6) Given the display-to-image correspondences, estimate the location and orientation of the normalized image plane in the calibration camera reference and calculate the effective focal distance, the center offset, and the distortion factor. In this step, we should obtain all the intrinsic parameters of EVP system and the rotation component R_E of the eye transformation in the calibration camera reference.
7) The eye transformation in the sensor reference is given by

$$T_{S\leftarrow E} = T_{S\leftarrow W_P} T_{W_P\leftarrow B}\, T_{B\leftarrow C} \begin{bmatrix} R_E & 0 \\ 0 & 1 \end{bmatrix} \quad (5)$$

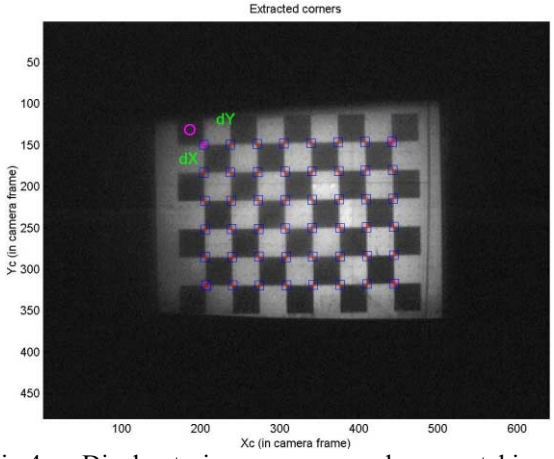

Fig.4 Display-to-image correspondence matching

It is important to note that the choice of camera calibration methods is critical. Theoretically, any image-based camera calibration methods can be used in our method. However, considering the limited accuracy of stylus measurement, Zhang's fast camera calibration method is recommended. In Zhang's method, the calibration points do not need to be transferred to one single coordinate system. Therefore, the error of tracker measurements has no effect on the calibration results before they are transferred to sensor coordinate. As a result, the accuracy of the intrinsic parameters is independent of the tracker accuracy. Furthermore, if we use same extra board to calibrate both eyes, the extrinsic estimates for the two eyes are equally disturbed by the tracker errors. Therefore, the relative position and orientation of the two viewing systems is not affected by the tracker accuracy.

In the calibration experiments, we used total 14 calibration boards to calibrate each of the cameras. Each board has total 140 points. Three extra calibration boards are used to calculate the transformation $T_{B\leftarrow C}$ and $T_{W\leftarrow B}$. Three LCD images are captured using the calibration camera for each eye. The display calibration pattern used to calculate the attitude of normalized image plane has total 8x10 points within the FOV of the calibration camera. The estimated intrinsic and extrinsic parameters are listed in Table I, corresponding to the left and right eyes, respectively:

$$[T_{S\leftarrow E}]_{Left} = \begin{bmatrix} 0.9913 & -0.0099 & 0.1316 & -3.7372 \\ -0.1301 & 0.0882 & 0.9876 & 20.617 \\ -0.0214 & -0.9961 & 0.0862 & -124.39 \\ 0 & 0 & 0 & 1 \end{bmatrix}$$

$$[T_{S\leftarrow E}]_{Right} = \begin{bmatrix} 0.9997 & -0.0187 & -0.0189 & 62.369 \\ 0.0202 & 0.0703 & 0.99732 & 23.436 \\ -0.0173 & -0.9974 & 0.0707 & -122.14 \\ 0 & 0 & 0 & 1 \end{bmatrix}$$

Table I Intrinsic and extrinsic parameters of the HMPD

Parameters	Left	Right
Focal length (mm)	35.368	34.905
FOV (degrees)	40.954(H) 31.292(V)	41.451 (H) 31.686(V)
Display offsets(pixel)	H=-24.24 V=3.42	H=-8.1979 V=17.347

5. Evaluation experiments and results

In this section, we will describe the experimental setup and method used to evaluate the ACM calibration method. Evaluation data are collected by a human subject who manually performs the world-to-image correspondence matching at the HMPD exit pupil. The experiment is applied on left eye only.

5.1. Experimental setup and procedures

In the experiments, the HMPD is mounted on an optical table. An evaluation target is placed in front of the HMPD about arm length away. The target is a 12x10 grid pattern with a pitch of 40mm. The grid line is 2mm wide. The subject is asked to look through HMPD and align computer-generated virtual cross with each of the real grid intersections. The corresponding points on the LCD are recorded by clicking left button of the mouse. Total nine attitudes with 1080 points are sampled. The attitude of each evaluation board is measured by stylus, which is used to transfer the grid intersections from the board coordinates to the world coordinates. The detailed procedure is as the following:

1) Position the evaluation target at a fixed attitude, record its grid coordinates using the Hiball stylus, and compute their coordinates in the world coordinates using the transformation $T_{W\leftarrow B}$.
2) Transfer the grid coordinates from world coordinates to eye coordinate using the matrix set obtained in calibration process, i. e., the eye transformation $\begin{bmatrix} R_E & 0 \\ 0 & 1 \end{bmatrix}^{-1} T_{B\to C}^{-1} T_{W\leftarrow B}^{-1}$. Please note that the footmark B here is referred as to the extra calibration board;
3) Project the grid coordinates from eye coordinates to the normalized plane using the projection matrix formed by the intrinsic parameters we obtained in the calibration process. We express these 2D points as $\hat{Q}_{i,j}^{k}(u,v)$.
4) Ask the subject to align a virtual cross with each of the grid intersections on the target, and record the corresponding pixel coordinates, $Q_{i,j}^{k}(u,v)$;
5) Compute the difference between the computed and the ground-truth projections: $e_{i,j}^{k}(u,v) = \left| Q_{i,j}^{k}(u,v) - \hat{Q}_{i,j}^{k}(u,v) \right|$;
6) Change the target attitude, and repeat the steps 1 through 5;
7) Evaluate the means and standard deviations (STDs) of the samples at all different attitudes.

5.2. Results and discussion

The accuracy of the display calibration relies on the accuracy of the world coordinate measurements, the accuracy of the correspondence matching, and the accuracy of calibration algorithm. In our experiments, the accuracy of the world coordinate measurements relies on that of the Hiball stylus. Due to the highly reflective environments in our system, the stylus has limited accuracy, between 2mm and 5mm, which corresponds to approximately 2- and 5-pixel error in the display space. Figures 5-a and 5-b show the mean and standard deviation of the projection errors, corresponding to the 9 different evaluation targets, in which the display parameters are estimated from three different LCD images. The mean errors are from 2 to 7 pixels, and this accuracy matches with that of the stylus. The difference of three curves in STD plot is less than 0.15 pixels and in mean plot is less than 0.3 pixels, which means that proposed method is fairly stable. Figures 5-c and 5-d show the error distributions corresponding to evaluation board #8 and #9, respectively. The display parameters are estimated from the first LCD image. In the plot 5-c, the overall computed points shift to the left compared with ground truth data, which is mainly caused by the error of stylus measurement. In fact, from other experiments, we already confirm that this group of board sample is much less accurate than other evaluation boards. In plot 5-d, we can see the computed points are fairly well overlapped with the ground truth points.

Another important error source is the calibration algorithm itself. Based on the analysis in the section 3, we know that these extrinsic and intrinsic parameters are closely related to the eye position. Actually, in practice, it is less likely that a user can align his eye with the position of the calibration camera. Therefore, some amount of systematic error exists in the proposed calibration method. For our HMPD prototype, the exit pupil diameter is 12mm, which means that the maximum offset from a user's eye to the calibrated eyepoint is less than 6mm. This upper bound will lead to around 3-pixel error in the display space, which is actually is smaller than the error caused by the current head tracker. When a

more precise registration is demanded, an on-line calibration is necessary after the off-line calibration.

6. Conclusion

This paper presents a fast and easy off-line calibration method for HMPD-based AR system. This method uses image-based method to sample data with sub-pixel accuracy, which minimizes the effect of the limited tracker accuracy on the calibration result. The evaluation results confirm that the method can achieve stable convergence with fairly good accuracy. The calibration method has limited accuracy because the variation of the eye location is not considered. However, compared with the accuracy limitation imposed by head tracker, the proposed method is able to work with most of the AR applications. We are developing a simplified on-line calibration method accompanying with the proposed off-line method.

Acknowledgements

We would like to specially thank our collaborators Dr. Jannick Rolland of the ODALab at the University of Central Florida for her stimulating discussion. We would also like to acknowledge 3M Inc. for supplying retro-reflective film. This paper is based on work supported by National Science Foundation Grant IIS 00-83037 ITR and Beckman Institute Equipment Allocations.

References

[1] Y. Argotti, L. Davis, V. Outters, and J. P. Rolland, "Dynamic superimposition of synthetic objects on rigid and simple-deformable real objects", *Proceedings of IEEE International Symposium on Augmented Reality 2001*, pp. 5-10, October 29-30, 2001, New York, NY.

[2] R. Azuma and G. Bishop, "Improving static and dynamic registration in an optical see-through display," *Computer Graphics (Proc. SIGGRAPH Conf.)*, pp. 194-204, July 1994.

[3] M. Bajura, H. Fuchs, and R. Ohbuchi, "Merging virtual objects with the real world: Seeing ultrasound imagery within the patient," *Computer Graphics (Proc. SIGGRAPH Conf.)*, pp203-210, Chicago, IL, July 1992.

[4] M. Bajura and U. Neumann. "Dynamic registration correction in augmented-reality systems," *Proc. Virtual Reality Ann. Int'l Symp. (VRAIS'95)*, pp189-196, Research Triangle Park, N.C., Mar. 1995.

[5] .T. Caudell and D. Mizell, "Augmented reality: An application of heads-up display technology to manual manufacturing processes," Proc. Hawaii Intl Conf. Systems Sciences, pp659-669, Jan 1992.

[6] Cruz-Neira, Carolina, Daniel Sandin, and Thomas

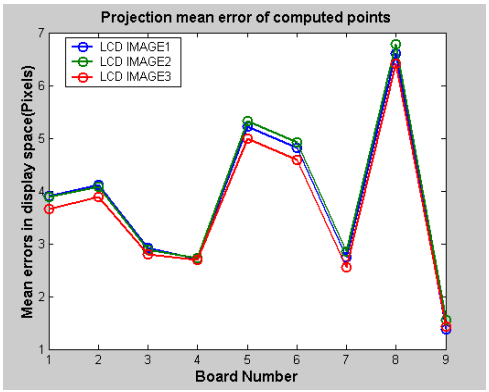

(a)

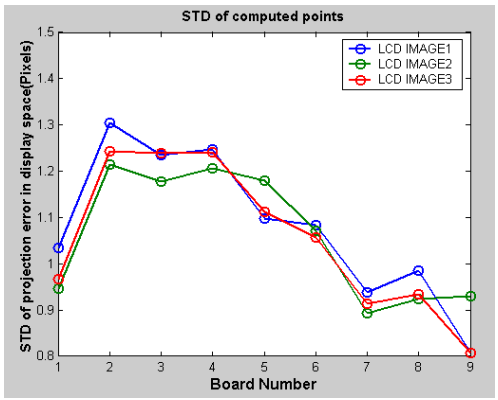

(b)

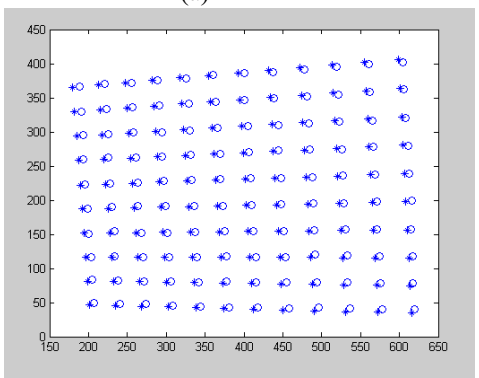

(c)

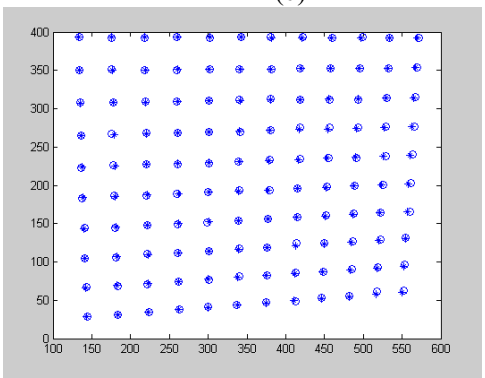

(d)

Fig. 5 Evaluation results: (a) Mean error of computed points; (b) STD of computed points; (c) Registration error distribution obtained from board 8; (d) Registration error distribution obtained from board 9.

Defanti. “Surround screen projection-based Virtual Reality: the design and implementation of the CAVE.” In *Proceedings of SIGGRAPH*, 135-142, Anaheim, CA, Aug 1993

[7] Michael Deering, High resolution virtual reality, Computer Graphics, Prof SIGGRAPH’92 Conf., 26(2), 195-202, July 1992

[8] J. Fergason. “Optical system for head mounted display using retro-reflector and method of displaying an image”, U.S. patent 5,621,572. April 15, 1997.

[9] S. Feiner, B. MacIntyre, and D. Seligmann, “Knowledge-based augmented reality,” Comm. ACM, 36(7): 53-62, July 1993.

[10] W. E. L. Grimson, G. J. Ettinger, S. J. White, T. Lozano-perez, W. M. Wells, and R. Kikinis. “ An automatic registration method for frameless sterertaxy, image guided surgery, and enhanced reality visualization,” IEEE Trans. On Medical Imaging, 15(2), 129-140, April 1996.

[11] Hong Hua, A. Girardot, Chunyu Gao, and J. P. Rolland. “Engineering of head-mounted projective displays”. *Applied Optics*, 39 (22), 2000, 3814-3824.

[12] Hong Hua, Chunyu Gao, Frank Biocca, and Jannick P. Rolland, "An Ultra-light and Compact Design and Implementation of Head-Mounted Projective Displays", *Proceedings of IEEE-VR 2001*, p. 175-182, March 12-17, 2001, Yokohama, Japan.

[13] Hong Hua, Chunyu Gao, Leonard Brown, Narendra Ahuja, and Jannick P. Rolland, “Using a head-mounted projective display in interactive augmented environments”, in *Proceedings of IEEE International Symposium on Augmented Reality 2001*, pp. 217-223, October 29-30, 2001, New York, NY.

[14] Hong Hua, Chunyu Gao, Leonard Brown, Narendra Ahuja and J. P. Rolland, “A Testbed for Precise Registration, Natural Occlusion and Interaction in an Augmented Environment Using a Head-Mounted Projective Display (HMPD),” in *IEEE VR 2002 Proceedings*, 81-89 Orlando, FL, March 22-28, 2002

[15] H. Hua, C. Gao, and N. Ahuja, “Calibration of a head-mounted projective display for augmented reality systems,” to appear in *Proceedings of IEEE International Symposium on Mixed and Augmented Reality 2002*, Darmstadt, Germany, Sep. 30-Oct. 1st, 2002.

[16] Masahiko Inami, Naoki Kawakami, Dairoki Sekiguchi, Yasuyuki Yanagida, Taro Maeda, and Susumu Tachi, “Visuo-haptic display using head-mounted projector”, *Proceedings IEEE Virtual Reality 2000*, IEEE Comput. Soc. 2000, pp.233-40. Los Alamitos, CA, USA.

[17] A. Janin, D. Mizell, and T. Caudell, “Calibration of head-mounted displays for augmented reality applications,” Proc Virtual Reality Ann. Int’l Symp, (VRAIS’93), pp246-255, Sept. 1993.

[18] Naoki Kawakami, Masahiko Inami, Dairoku Sekiguchi, Yasuyuki Yangagida, Taro Maeda, and Susumu Tachi, “Object-oriented displays: a new type of display systems—from immersive display to object-oriented displays”, *IEEE SMC'99 Conference Proceedings*, 1999 IEEE International Conference on Systems, Man, and Cybernetics, Vol.5, 1999, pp.1066-9 vol.5. Piscataway, NJ, USA.

[19] Ryugo Kijima and Takeo Ojika, “Transition between virtual environment and workstation environment with projective head-mounted display”, *Proceedings of IEEE 1997 Virtual Reality Annual International Symposium,* IEEE Comput. Soc. Press. 1997, pp.130-7. Los Alamitos, CA, USA.

[20] W. Lorensen, H. Cline, C. Nafis, R. Kikinis, D. Altobelli, and L. Gleason, “Enhancing reality in the operating room,” Proc. Visualization’93 Conf., pp. 410-415, Los Alamitos, CA., Oct. 1993.

[21] P. Milgram, S. Zhai, D. Drascic, and J. J. Grodski, “Applications of augmented reality for human-robot communication,” Proc. IROS’93: Int’l Conf. Intelligent Robots and Systems, pp1467-1472, Yokohama, July 1993.(Search for recent)

[22] Takashi Oishi and Susumu Tachi, “Methods to calibrate projection transformation parameters for see-through head-mounted displays,” Presence: *Teleoperators and Virtual Environments (MIT Press), 5(1), 122-135, 1996.*

[23] J. Parsons, and J. P. Rolland, “A non-intrusive display technique for providing real-time data within a surgeons critical area of interest,” *Proceedings of Medicine Meets Virtual Reality98*, 1998, 246-251.

[24] J. P. Rolland, and H. Fuchs, "Optical versus video see-through head-mounted displays in medical visualization," *Presence: Teleoperators and Virtual Environments (MIT Press),* 9(3), (2000), 287-309.

[25] Roger Y. Tsai. “A versatile Camera Calibration Technique for High-Accuracy 3D Machine Vision Metrology Using Off-the-Shelf TV Cameras and Lenses”, *IEEE Journal of Robotics and Automation*, Vol. RA-3, No. 4, August 1987, pages 323-344.

[26] Mihran Tuceryan, et al. “Calibration requirements and procedures for a monitor-based augmented reality system,” IEEE Trans. Visualization and Computer Graphics, 1(3): 255-273, Sep. 1995.

[27] Mihran Tuceryan, Nassir Navab. “Single point active alignment method (SPAAM) for optical see-through HMD calibration AR,” In *Proceedings of IEEE International Symposium on Augmented Reality 2000*, pp. 149-157, 2000.

[28] Z. Zhang. "A flexible new technique for camera calibration". *IEEE Transactions on Pattern Analysis and Machine Intelligence, 22(11):1330-1334, 2000*.

[29] Camera calibration toolbox for matlab http://www.vision.caltech.edu/bouguetj/calib_doc/.